7 Dynamo and convection experiments

Henri-Claude Nataf

LGIT, Université Joseph-Fourier de Grenoble, BP53, 38041 Grenoble Cedex 9, France

Year 2000 was marked by the success of the dynamo experiments of Riga and Karlsruhe. In both cases, a saturated magnetic field of a few milliTeslas was produced. These successes crown years of efforts of the two teams during which the experiments were planned, built and tested. In both cases, more than a cubic meter of liquid sodium is used and the flow is driven into a well-defined configuration with powers in excess of 100 kW. The configurations were chosen to mimic known kinematic dynamos, thus enabling a good prediction of the onset of dynamo action. These experiments demonstrate the feasibility of laboratory dynamos and open the way to a second generation of experiments, in which the flow will have more freedom to organize itself under the combined actions of the forcing and of the Lorentz force. It will also be interesting to explore the effect of the Coriolis force and to unravel the characteristics of turbulence in these dynamos. All these dynamo experiments nicely complement the numerical models now available because they allow the exploration of regimes with low magnetic Prandtl number and high Reynolds number.

I also review laboratory experiments that aim at the understanding of convection in planetary cores. There also, turbulent regimes are more easily reached than in numerical experiments, and new features have been discovered recently. Crystallization experiments explore a new class of mechanisms with implications for the anisotropy of the inner core.

Experiments continue to play an important role in the modelling of mantle convection, as illustrated by the recent findings on the organization of convection in two superposed layers. New types of behaviours are being investigated, with emphasis on nonlinear physics and dynamical systems.

1. Introduction

This chapter focuses on laboratory experiments that have been carried out recently to help understand the dynamics of the Earth's deep interior. Experiments have always played a major role in fluid mechanics. Before computers became available, experiments were the main providers of ideas and data. Now that numerical modelling has become the powerful tool that we know, experiments continue to play a unique role in fluid mechanics.

They often complement the parameter space available for numerical modelling. For example, we will see that the very low values of the magnetic Prandtl number P_m ($P_m = \nu/\eta$, where ν is the kinematic viscosity and η the magnetic diffusivity) expected for liquid iron in the Earth's core cannot be reached in numerical models, while they are typical of liquid metals such as gallium and sodium that are used in laboratory experiments.

Another nice thing about experiments is that they force the realization of physically realistic situations. If a magnetic field is imposed, it has to be produced by a magnet or by a coil in

some physical way. Boundaries, which often play a key role in the dynamics of rotating fluids, have to be present as well in an actual experiment.

Even more interesting is the fact that experiments often give another viewpoint. The problem of precession, discussed by Aldridge in Chapter 8 of this volume provides a striking illustration of this remark: while flow in a precessing sphere seems dominated by shear on geostrophic cylinders in laboratory experiments, the most conspicuous features in numerical models are inclined bands of oscillatory motions. It is only very recently that the two viewpoints have been shown to be two facets of the same complex phenomenon. The common sense intuition is indeed often defeated when dealing with rotating fluids, and even more when a magnetic field is present. Experiments certainly help improve our physical appraisal of what is going on.

While the explosion of computer resources clearly plays a central role in the fascinating progression of numerical modelling, it is not always realized that, together with other technological improvements, they have also considerably enriched the output of experiments. New measuring techniques, such as particle image velocimetry (PIV) or ultrasonic Doppler velocimetry, are available and large quantities of data can now be handled and processed easily in the lab. New technologies have also appeared. For example, the use of liquid sodium in the nuclear industry has led to a much better knowledge of its properties and handling requirements, and this is very valuable for scientists that design dynamo experiments today.

Finally, I note that the widespread availability of computer resources and numerical codes makes it possible for a small group of investigators to carry on experiments and numerical simulations together. Several teams in the world operate in this fashion, and this appears to be very fruitful.

The event of year 2000 was the success of two dynamo experiments, and the first section of this chapter is devoted to these experiments. The main results are reviewed, with emphasis on the new questions that arise, opening the way to a new generation of dynamo experiments. I then discuss recent experimental findings concerning convection in the Earth's core – including crystallization – and in the Earth's mantle.

2. Dynamo experiments

Following the ideas of Larmor (1919), Elsasser (1946) and Bullard and Gellman (1954), it is now widely accepted that the magnetic field of the Earth is sustained by some sort of dynamo mechanism in its metallic liquid iron core (see Busse *et al.* in Chapter 6 of this volume). Consider the induction equation in a continuum:

$$\frac{\partial \mathbf{B}}{\partial t} + \nabla \times (\mathbf{B} \times \mathbf{u}) = \eta \nabla^2 \mathbf{B}. \tag{1}$$

For suitable imposed velocity fields $\mathbf{u}$, the solution $\mathbf{B} = \mathbf{0}$ is unstable and a magnetic field appears and grows when the magnetic Reynolds number $R_\mathrm{m} = UD/\eta$ is large enough, where U is a typical velocity and D a typical length. For a given velocity field, it is possible to evaluate the critical magnetic Reynolds number $R_{\mathrm{m}_\mathrm{c}}$ of instability: this is the basis of the kinematic dynamo approach.

One of the first tasks of the proponents of the dynamo mechanism was to find velocity fields that could act as a dynamo. Among the various solutions found, three have now found an experimental counterpart (see Lielausis, 1994 and Tilgner, 2000 for recent reviews on experimental dynamos).

Table 1 Physical properties of a few liquids used in the experiments

Property	*Symbol*	*Unit*	*Sodium*, 200°C	*Gallium*, 30°C	*Water*, 20°C
Density	ρ	$kg\,m^{-3}$	910	6,095	1,000
Kinematic viscosity	ν	$m^2\,s^{-1}$	5×10^{-7}	2.95×10^{-7}	10^{-6}
Coefficient of thermal expansion	α	K^{-1}	2.9×10^{-4}	1.26×10^{-4}	2×10^{-4}
Thermal conductivity	k	$W\,m^{-1}\,K^{-1}$	82	30	0.59
Heat capacity	C_p	$J\,K^{-1}\,kg^{-1}$	1,330	381	4,180
Thermal diffusivity	κ	$m^2\,s^{-1}$	0.66×10^{-4}	1.3×10^{-5}	1.4×10^{-7}
Electric conductivity	σ	$\Omega^{-1}\,m^{-1}$	7.5×10^6	3.87×10^6	–
Magnetic diffusivity (at 150°C)	η	$m^2\,s^{-1}$	0.106 (0.092)	0.21	–
	$\rho\eta^3$	W m	1.08	53	–
Prandtl number	Pr	ν/κ	7.5×10^{-3}	0.023	7.1
Magnetic Prandtl number	P_m	ν/η	4.7×10^{-6}	1.4×10^{-6}	–

The first experimental dynamo was built by Lowes and Wilkinson (1963, 1968). It was inspired from the kinematic dynamo of Herzenberg (1958) and nicely depicted the phenomenon of reversals. Two solid cylinders were rotated around nonparallel axes. Mercury provided electrical continuity between the two cylinders. The device did work as a dynamo because the cylinders were made of ferromagnetic iron, with a very low magnetic diffusivity, thus enabling large magnetic Reynolds numbers to be reached for moderate size and velocity.

The two other kinematic dynamos that have inspired actual experiments are those of Ponomarenko (1973) and Roberts (1972). They provide a theoretical guide to the experiments of Riga and Karlsruhe, respectively. These two experiments are homogeneous liquid dynamos and no ferromagnetic part is present.

All the experimental dynamos described below use liquid sodium as a working liquid, because of its low magnetic diffusivity and low density. The relevant physical properties of liquid sodium are given in Table 1. Note that the magnetic diffusivity of liquid sodium increases with temperature. Hence, dynamo action is more easily reached at low temperature (but freezing of sodium – at 98°C – is to be avoided!).

2.1. The Riga dynamo experiment

The success of the Riga dynamo in year 2000 crowns 30 years of efforts under the guidance of Professor Agris Gailitis. The set-up of the dynamo, shown in Figure 1, was designed by the Riga group to mimic the Ponomarenko (1973) kinematic dynamo. The dynamo module is a 3 m long cylinder, containing about 1.5 m^3 of liquid sodium, split into three co-axial cylindrical volumes. In the inner cylinder (0.25 m in diameter), liquid sodium flows down in a helicoidal fashion, forced by a propeller at the top. The return flow takes place vertically between the inner tube and the surrounding one. The outermost shell of sodium is at rest. The propeller is driven at up to 2,200 rpm by two 55 kW electric motors. The expected eigenmode for the magnetic field consists in a vector field that also follows an helice and oscillates in time at a given position. The critical magnetic Reynolds number was determined by Ponomarenko (1973) for an infinitely long cylinder. Gailitis and Freibergs (1976) computed the threshold in a finite cylinder for both the convective and the absolute instability.

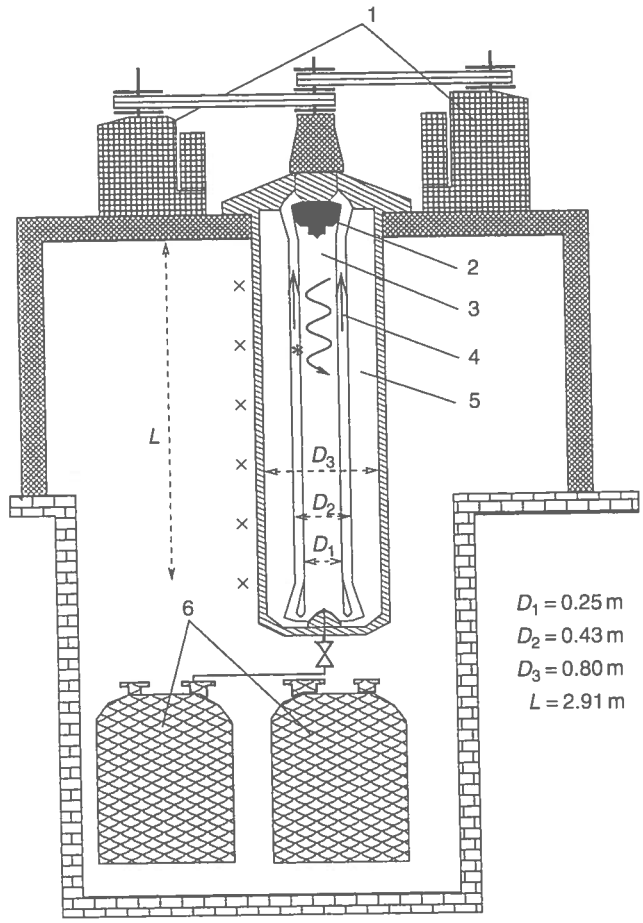

Figure 1 The Riga dynamo facility. Main parts are: 1 – two motors (55 kW each), 2 – propeller, 3 – helicoidal flow region, 4 – back-flow region, 5 – sodium at rest, 6 – sodium storage tanks, ∗ – position of the flux–gate sensor and the induction coil, × – Positions of the Hall sensors. (Reprinted with permission from Gailitis, A. *et al.*, "Detection of a flow induced magnetic field eigenmode in the Riga dynamo facility," *Phys. Rev. Lett.* **84**, 4365–4368 (2000). Copyright (2000) by the American Physical Society.)

In 1987, measurements of the decay rate of an applied magnetic field showed that the predicted threshold was correct and could be reached in the experiment (Gailitis *et al.*, 1987). However, mechanical vibrations in the set-up forced the experiment to a stop.

The module was built anew and the propeller redesigned to drive an optimal flow, and in November 1999, the Riga group observed the slow growth of a magnetic eigenmode for a few seconds before the experiment had to be stopped again because of a sealing problem (Gailitis *et al.*, 2000). Figure 2 shows the actual record of the magnetic field. A 1-s period field was applied, and the beating observed in the record indicates that a signal with a 1.3-s period is slowly growing. This phenomenon was observed for a rotation rate of about 2,150 rpm and

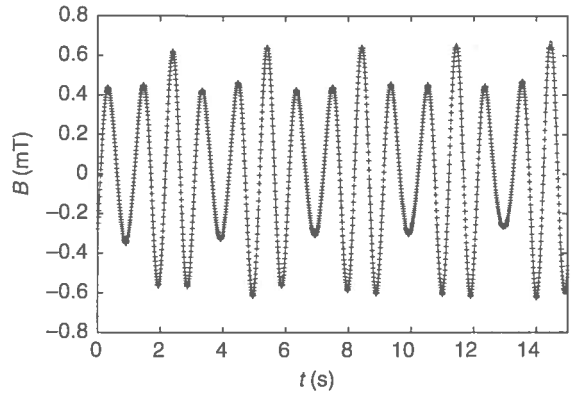

Figure 2 Growth of a magnetic eigenmode of the Riga dynamo. The magnetic field measured by the flux-gate sensor (see Figure 1) in November 1999 for a rotation rate of 2,150 rpm. Note that the imposed 1 Hz signal beats with a growing 1.3 Hz eigenmode. (Reprinted with permission from Gailitis, A. *et al.*, "Detection of a flow induced magnetic field eigenmode in the Riga dynamo facility," *Phys. Rev. Lett.* **84**, 4365–4368 (2000). Copyright (2000) by the American Physical Society.)

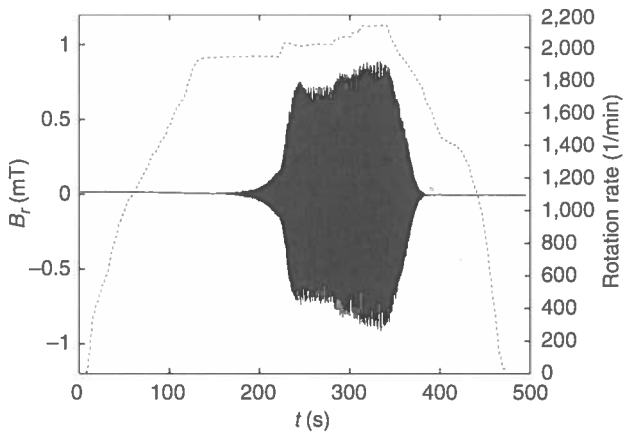

Figure 3 Saturation of the magnetic field in the Riga dynamo. The magnetic field is the continuous line with the scale at the left, while the dotted line gives the variation of the rotation rate (scale on the right) as a function of time during the experiment. Note that as the rotation rate approaches 1,950 rpm, an alternating magnetic field starts growing. At saturation, its amplitude follows the small variations of the rotation rate and then drops when the latter is reduced below the threshold. (Reprinted with permission from Gailitis, A. *et al.*, "Magnetic field saturation in the Riga dynamo experiment," *Phys. Rev. Lett.* **86**, 3024–3027 (2001). Copyright (2001) by the American Physical Society.)

when the temperature of the sodium was about 200°C. The growth rate and the frequency of the magnetic eigenmode are in good agreement with the theoretical predictions.

In July 2000, after the seal was replaced, a series of new runs were conducted with sodium at a temperature of about 160°C. This time, as shown in Figure 3, the magnetic eigenmode

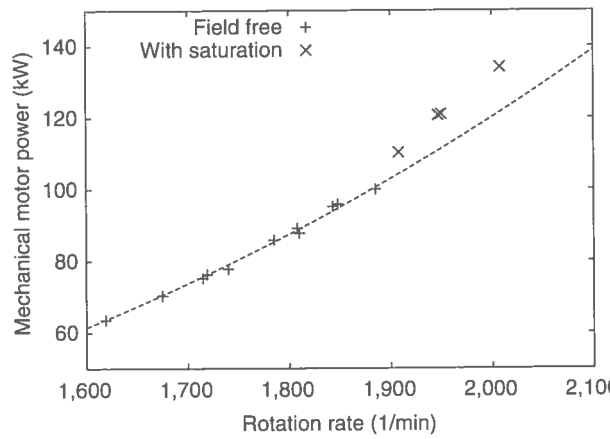

Figure 4 Motor power (in kW) as a function of the rotation rate of the propeller in the Riga experiment, below (+) and in (×) the dynamo regime. Power scales as rotation rate to the third power (dashed line) below the dynamo regime. (Reprinted with permission from Gailitis, A. *et al.*, "Magnetic field saturation in the Riga dynamo experiment," *Phys. Rev. Lett.* **86**, 3024–3027 (2001). Copyright (2001) by the American Physical Society.)

could grow up to saturation levels of a few milliTeslas, and remain at that level for several minutes (Gailitis *et al.*, 2001). As expected, the power increases as rotation rate to the third power below the onset of the dynamo. Once the magnetic field is present, the power needed to sustain a given rotation rate is increased by up to 10 kW, and dissipates in Joule heating (see Figure 4). Measurements of the magnetic field in this regime reveal that the flow is modified by the presence of the magnetic field: velocities decrease from the top to the bottom of the apparatus. *In situ* velocity measurements would help corroborating this observation.

2.2. The Karlsruhe dynamo experiment

The Karlsruhe experiment (Busse *et al.*, 1998a) was built to model another kinematic dynamo: the two-scale periodic dynamo of Roberts (1972). Figure 5 gives a schematic view of the actual dynamo module. A 1.7 m diameter, 0.85 m high cylinder is paved with fifty-two 'spin-generators'. Each of these spin-generators consists of two parts: a 10 cm diameter inner tube inside a 21 cm diameter outer tube with helicoidal blades. Liquid sodium is driven in both the inner and outer tube circuits with separate external magnetohydrodynamic pumps at volumetric rates of about $110\,m^3\,h^{-1}$. The gaps between generators are filled with sodium at rest. Roberts showed that an infinite pattern of such bidimensional periodic flow could create a large-scale magnetic field. The threshold for dynamo action was calculated for the finite configuration by Tilgner (1997) and Rädler *et al.* (1998). The magnetic field fastest growing eigenmode is predominantly horizontal and rotates by π from the top to the bottom of the dynamo module.

In the meantime, the dynamo module was built by the group of Professor Müller and Stieglitz in the Institute for Nuclear and Energy Technologies in Karlsruhe (see Figure 6).

In December 1999, the dynamo was run and a magnetic field was indeed produced (Stieglitz and Müller, 2001). A steady field of intensity up to 16 mT was observed. The field could be maintained for more than 10 min. The onset of dynamo action was obtained for flow rates

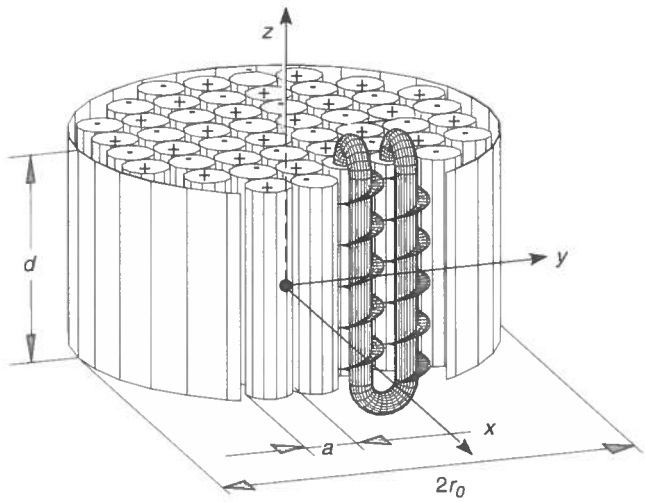

Figure 5 Sketch of the dynamo module of the Karlsruhe experiment. Fifty-two spin-generators are packed inside a 1.7 m diameter cylinder. The inner structure is shown for two spin-generators in the front row. The signs indicate the direction of the sodium flow in individual spin-generators. (Reprinted with permission from Stieglitz, R. and Müller, U., "Experimental demonstration of a homogeneous two-scale dynamo," *Phys. Fluids* **13**, 561–564 (2001). Copyright (2001) by the American Physical Society.)

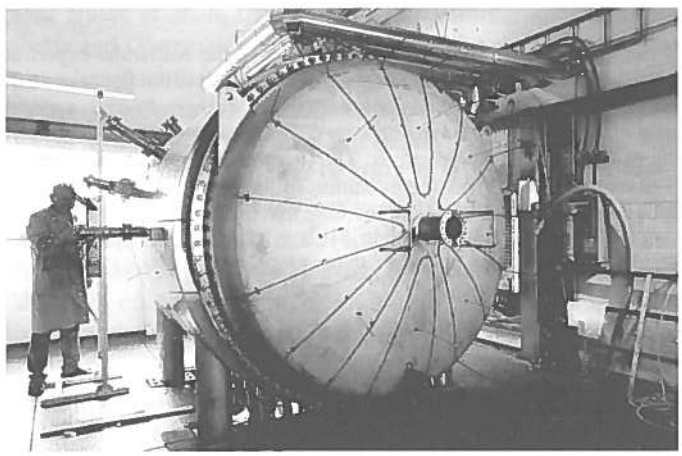

Figure 6 Photograph of the dynamo module of the Karlsruhe experiment. (Courtesy of Professor Müller.)

slightly above 100 $m^3\,h^{-1}$ with liquid sodium at a temperature of 125°C. The threshold thus appears to be somewhat lower than in the theoretical predictions (Figure 7). In the year 2000, more runs were performed. The geometry of the magnetic field was found to be in good agreement with the predictions, but could depend on the initial electromagnetic conditions. More attention was given to the saturation mechanism. One could have thought that once the

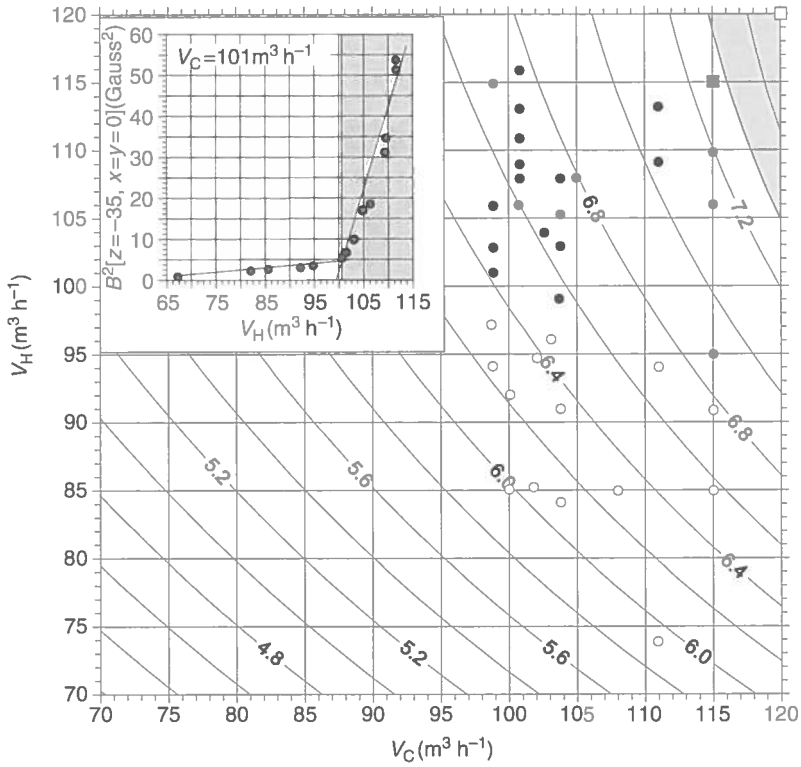

Figure 7 Stability diagram for the onset of dynamo action in the Karlsruhe experiment. V_C is the flow rate in the central part of the spin-generators and V_H is the flow rate in their helicoidal outer part (see Figure 5). The filled circles are for runs where dynamo action was observed, while open circles denote nondynamo states. The grey area specifies the dynamo domain according to Rädler *et al.*'s predictions. The two squares indicate Tilgner's predictions for dynamo onset. The inset gives the evolution of the magnetic energy as a function of V_H when V_C is held fixed. Note the sharp increase that marks the dynamo onset (grey domain). (Reprinted with permission from Stieglitz, R. and Müller, U., "Experimental demonstration of a homogeneous two-scale dynamo," *Phys. Fluids* **13**, 561–564 (2001). Copyright (2001) by the American Physical Society.)

magnetic field has appeared, an increase in the pressure head in the pumps will only increase the magnetic field and leave the velocity field unchanged (Busse *et al.*, 1998a). Instead, it appears that the flow rate continue to increase above the dynamo threshold. Tilgner and Busse (2001) interpret this as an indication that the Lorentz force, which grows as the magnitude of the magnetic field increases, does not simply reduce the amplitude of the liquid sodium flow but also modifies the velocity field in some way. *In situ* velocity measurements would help understanding this phenomenon.

It is clear that the success of the dynamo experiments in Riga and Karlsruhe represent a key milestone. It provides an experimental validation of the kinematic dynamo approach. It shows that such experiments are feasible, as impressive and difficult as they might look. In the two experiments, the flow is turbulent since the Reynolds number reaches several

millions. However, the mean flow is much larger than its fluctuations. The Riga experiment demonstrates that, at the attained saturation level of the magnetic field, the Lorentz force does not modify the mean flow drastically. Clearly, it would be interesting to monitor the velocity field in this situation. The Karlsruhe experiment demonstrates the efficiency of the separation of scales (small-scale velocity field creating a large-scale magnetic field). The two configurations were chosen because a magnetic field was predicted to appear for 'low' values of the magnetic Reynolds number. Nevertheless, both experiments need more than a cubic meter of sodium and dissipate powers of more than 100 kW. Future dynamo experiments will probably have similar requirements.

2.3. Turbulent dynamos

Indeed, a second generation of experimental dynamos is under way. The force of the 'kinematic' dynamo approach of Riga and Karlsruhe was to yield robust predictions for the dynamo threshold. Its main weakness is that the Lorentz force is not allowed to modify the mean flow in a strong way. This has lead several teams to propose new dynamo set-ups, in which the forcing is much less geometrically constrained.

2.3.1. Convective dynamos?

A typical example would be a convective dynamo: convective motions appear spontaneously once a sufficient temperature gradient is imposed, and when the convective velocities are large enough, a magnetic field can be created and is able to modify the geometry of the convective cells. This approach was followed with great success by numerical modellers in the recent years, but for hypothetical materials with physical properties far from those of liquid metals (see Busse *et al.* in Chapter 6 of this volume, and recent reviews by Fearn (1998) and Roberts and Glatzmaier (2000)). A convective dynamo is probably not feasible in the lab. If we extrapolate the scaling laws recently derived for the convective velocities in a rotating sphere filled with liquid gallium (see below), we get that typical convective velocities would be of only $0.1\,\mathrm{m\,s^{-1}}$ in a 1 m radius sphere rotating at 200 rpm and filled with liquid sodium when a thermal power of 100 kW is driving convection. Such velocities are probably two orders of magnitude too low to enable the growth of a magnetic field. After the early experiments of Dan Lathrop at the University of Maryland (Peffley *et al.*, 2000b), a similar conclusion was reached by Glatzmaier (2000). Nevertheless, Lathrop is presently conducting a 'dynamo' convection experiment in a 60 cm diameter sphere filled with liquid sodium, spinning at up to 6,000 rpm, with a driving thermal power of 10 kW. The challenge remains tantalizing, especially since doubts have been cast on the possibility of convective dynamo action in a low Prandtl number liquid (Busse *et al.*, 1998b).

2.3.2. Mechanical dynamos

Most investigators (including Lathrop) pursue another, more reachable, goal. The idea is to force fluid motions in a more efficient way by spinning some propeller in a tank filled with liquid sodium. Several features of the convective dynamo would be retained. In particular, the Lorentz force could strongly modify both the mean flow and its fluctuations. For dynamo action to take place, the magnetic Reynolds number must be high (of the order of 50?), hence the usual Reynolds number must be very high (larger than 10^7). As a consequence, it becomes very difficult to predict the onset of dynamo action. Indeed, only simple and stationary flows

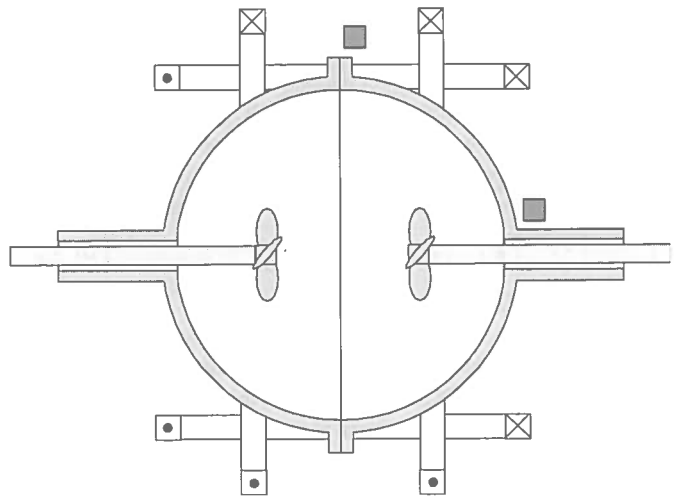

Figure 8 Schematic cross-section of the 'dynamo II' experiment at the University of Maryland. A 30 cm diameter sphere is filled with liquid sodium. Two propellers apply forcing and baffles enhance the poloidal flow. Also drawn are the magnetic coils that supply external magnetic fields and the two positions of the magnetometer. (Reprinted with permission from Peffley, N. L. *et al.*, "Toward a self-generating magnetic dynamo: the role of turbulence," *Phys. Rev. E* **61**, 5287–5294 (2000). Copyright (2000) by the American Physical Society.)

are easily tested with the kinematic dynamo approach, and the onset of dynamo action is then found to be very sensitive to details of the imposed velocity field. Furthermore, in contrast to the onset of convection in most situations, an increase in the control parameter (the amplitude of velocity) can lead to a decrease of the growth rate of a seed magnetic field. Entering the dynamo regime in this configuration could therefore be very different from what is seen in the dynamos of Riga and Karlsruhe. In fact, there is no guarantee that a given forcing will ever produce a dynamo!

Since it is difficult to predict the dynamo onset of a turbulent dynamo using the kinematic dynamo approach, some efforts have been put in determining it experimentally in small size experiments. The approach was pioneered by Lathrop (Peffley *et al.*, 2000a). Figure 8 shows the set-up he built. Two propellers along the same polar axis spin in opposite senses inside a 30 cm diameter sphere filled with liquid sodium. One expects a flow with a strong azimuthal component and a meridional circulation, both antisymmetric with respect to the equator. One of the most interesting results obtained by Lathrop is shown in Figure 9. In order to estimate how far from the onset he was, he monitored the growth rate of a pulse of magnetic field, in a similar way to Gailitis *et al.* (1987). When the propellers are at rest, the magnetic field growth rate is negative and its amplitude is given by the inverse of the magnetic diffusion time. When the propellers spin, the advection of the magnetic field by the flow can lead to an increase or a decrease of the growth rate. The dynamo onset corresponds to a zero growth rate. In addition, the growth rate depends on the geometry of the magnetic field. Lathrop tested two different geometries: an axisymmetric ($m = 0$) field and a $m = 1$ field pointing in a direction perpendicular to the rotation axis. While one could expect the latter to be the fastest growing mode, based on the similitude of the mean flow with axisymmetric $s_2 + t_2$ flows tested by Dudley and James (1989), the measurements indicate that, on the contrary, the

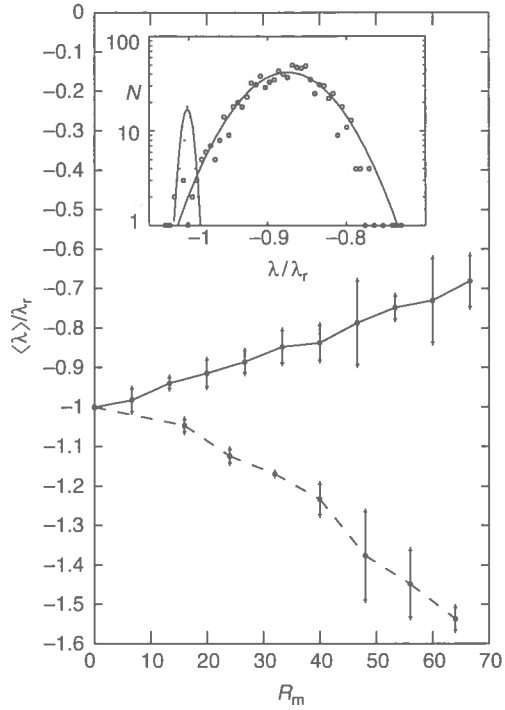

Figure 9 Growth rate λ of the magnetic field as a function of magnetic Reynolds number in the 'dynamo II' experiment of the University of Maryland. It shows a shift toward self-generation for fields aligned with the shafts ($m = 0$) (solid line) and a shift away from self-generation for fields at right angle ($m = 1$) (dashed line). The error bars indicate shot-to-shot fluctuations in the growth rate estimates. These fluctuations are further quantified by the distribution shown in the inset for 895 observations of the growth rate at the same $R_m = 42$. All the growth rates in this figure are normalized to yield -1 in conditions of no flow. The distribution for no flow $R_m = 0$ is the narrow Gaussian around -1 in the inset. Presumably, self-generation state is achieved when the $\lambda = 0$ line is crossed. (Reprinted with permission from Peffley, N. L. *et al.*, "Toward a self-generating magnetic dynamo: the role of turbulence," *Phys. Rev. E* **61**, 5287–5294 (2000). Copyright (2000) by the American Physical Society.)

$m = 1$ field decays more rapidly when the velocity increases. In contrast, the axisymmetric mode (which would always decay for a purely axisymmetric flow, under Cowling's (1934) theorem) decays less rapidly when motion is present. The inset also shows that in a turbulent flow, the distribution of instantaneous growth rates is very wide.

2.3.3. Small dynamos?

Several teams count on 'small' size experiments to reach the dynamo regime. Indeed, since the Reynolds number is linear in both size and velocity, one can choose to increase flow velocity rather than size, especially if one bears in mind that the volume of the experiment varies as the size to the power three. Following this idea, dynamo experiments with sodium volumes of less than 1001 have been designed and run by Lathrop (Peffley *et al.*, 2000a)

and by the French VKS group in Cadarache (Bourgoin *et al.*, 2001). The approach is also followed by the New Mexico group with 150 l (Colgate *et al.*, 2001a,b). These experiments are very interesting but they have not produced a dynamo yet. A simple argument helps understanding why. In the turbulent regime, the power needed to drive a flow scales as:

$$P \sim \rho\eta^3 \frac{R_m^3}{D}. \tag{2}$$

For a given flow, in order to reach the R_m needed for dynamo onset, a smaller experiment will need a higher driving power, hence a much higher power density. The difficulty is not so much in providing the power but rather in getting the heat out. It is indeed necessary to remove heat because otherwise the temperature would increase and the conductivity of sodium decrease, thus inhibiting dynamo action. With a volume of 70 l, optimized propellers and a driving power of 150 kW, the VKS group could not make a dynamo (Bourgoin *et al.*, 2001). Indeed, one may infer from their results that a driving power of 300 kW is needed for dynamo onset. Similar values are also obtained when extrapolating the growth rate curve of Lathrop in Figure 9. In other words, there is no such thing as a 'small dynamo', unless one is ready to call a Formula 1 race car a small car. Note that the $\rho\eta^3$ factor in Eq. (2) explains why all dynamo experiments use liquid sodium. This factor is about 1 W m for sodium (see Table 1) while it reaches 50 for gallium and 10,000 for mercury!

With 500 l of liquid sodium and a power of 200 kW, Forest (1998) of the University of Wisconsin at Madison has a chance to observe the dynamo onset once his set-up is operational. Another approach is followed by the Perm group, who investigates the onset of dynamo action in a transient flow (Frick *et al.*, 2000). The idea is to store a large kinetic energy in a 1 m diameter torus filled with 100 l of liquid sodium by spinning it at velocities up to 3,000 rpm. By bringing the torus to a stop very rapidly (in less than 0.1 s), one obtains very large flow velocities and a large transient power release, which might give rise to transient dynamo action.

It is clear that the involvement of physicists in dynamo experiments is rapidly increasing. This is rather natural if one considers the many fundamental issues still to be addressed concerning dynamo action. The expertise on handling liquid sodium acquired by the nuclear industry in the past 30 years is of great help in this enterprise. The experiments now underway have already brought valuable contributions; they have also prompted new questions. For example, how appropriate is the kinematic dynamo approach for predicting the onset of dynamo action in a turbulent flow? Will the onset correspond to a simple direct bifurcation as observed in the Riga and Karlsruhe dynamos, or be intermittent or super-critical (Sweet *et al.*, 2001)?

2.3.4. Geophysical dynamos?

While the geophysical community is clearly playing a leading role in numerical dynamos, its involvement in experimental dynamos is very limited. However, there are a number of issues for which dynamo experiments should prove fundamental. Many of these involve the effect of the Coriolis force. For example, will the Coriolis force help in getting dynamo action? This is a worthy hypothesis, considering that the onset of convection is lowered when both a magnetic field and rotation are present (see later). Another hint stems from the observation that heat transfer is enhanced in numerical models of convective dynamos when the magnetic field is present (Christensen *et al.*, 1999; Grote *et al.*, 2000). Other questions related to the dipolar geometry of the magnetic field and to possible inversions are also of great interest

for the geophysical community. Finally, the organization of turbulence in a turbulent rotating dynamo is central to the extrapolation of current numerical models to core conditions, while the power consumption of such a dynamo is important for models of the thermal history of the Earth.

These questions prompted our team in Grenoble to propose a set-up of a 'magnetostrophic dynamo' (Jault *et al.*, 1998). While the project is described elsewhere in more details (Cardin *et al.*, 2002), I just indicate that the idea is to spin a sphere filled with some $4\,\mathrm{m}^3$ of liquid sodium and to force some kind of internal motions by rotating an inner sphere or some other device. For a large enough power input (250 kW as a first estimate), it is expected that a strong magnetic field will appear, such that the Coriolis force will balance the Lorentz force. Most of the dissipation will take place by Joule heating in this regime. Again, since the flow will be very turbulent it is not easy to predict the onset of dynamo for a given forcing. And it is even more difficult to guess what flow will be produced once the magnetic field is acting. For these reasons, as well as for testing several technological issues, a smaller scale experiment has been constructed. A 60 cm diameter sphere filled with 40 l of liquid sodium is entrained by a 10 kW motor to rotation rates up to 2,000 rpm. A 20 cm diameter inner sphere is entrained by another 10 kW motor at a different rotation rate. The inner sphere is made of a permanent magnet, yielding a magnetic field of more than 0.1 T in the liquid, so that the organization of the flow in the presence of both rotation and magnetic field can be investigated.

3. Core convection experiments

We have seen that it was unlikely that a convective dynamo could be produced in the lab. On the other hand, numerical models of convective dynamos now exist (see Busse *et al.* in Chapter 6 of this volume) but for liquids with properties that are very different from what we expect for the Earth's core. In particular, it is very difficult to model liquids with a low Prandtl number $Pr = \nu/\kappa$ or a low magnetic Prandtl number $P_\mathrm{m} = \nu/\eta$. The organization of convective flows and dynamo action could be very different in this parameter regime. In fact, it has been suggested that dynamo action was not possible for low Prandtl numbers (Busse *et al.*, 1998b). It is therefore important to investigate the properties of convection for a wide range of parameters and try to understand better its characteristics, in the presence of rotation and with a magnetic field, even if the magnetic field is not produced internally by dynamo action. Several interesting results have been recently obtained along these lines.

3.1. Rayleigh–Bénard convection with rotation and a magnetic field

Chandrasekhar's (1961) famous monograph on hydrodynamic and hydromagnetic stability still serves as a reference on these questions. Of particular interest is the stability of an electrically conductive liquid layer between two horizontal plates at different temperatures, subject to rotation around a vertical axis and to a magnetic field in the same direction. When acting separately, both rotation and the magnetic field stabilize the fluid layer against convection. However, the marginal stability analysis of Chandrasekhar predicted that when rotation is present, adding a magnetic field destabilizes the fluid! A minimum of the critical Rayleigh number is obtained when the ratio of the Lorentz forces over the Coriolis forces (the Elsasser number) is of order one. This was confirmed by the pioneer experiments performed by Nakagawa (1957, 1958) with a layer of mercury placed inside a reconditioned cyclotron. The idea that the presence of the magnetic field could enhance convection when rotation is present has been rather influential in the past decades. It lead to the idea that convection

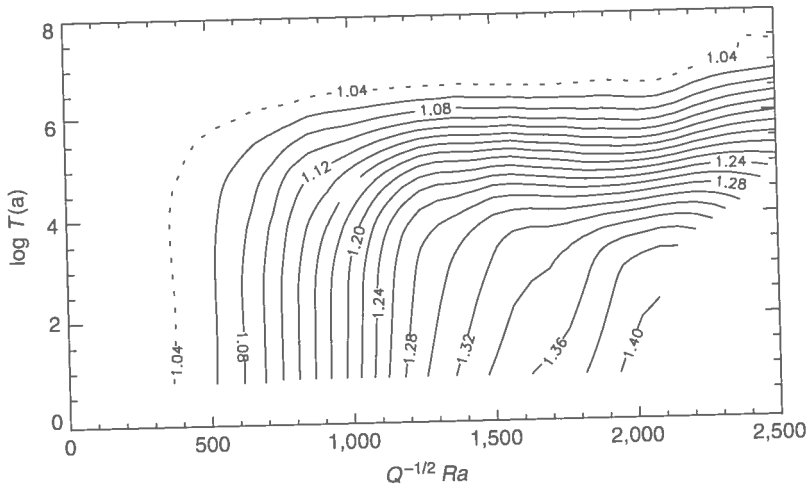

Figure 10 Isocontours of the Nusselt number for Rayleigh–Bénard convection in a horizontal layer of gallium in the presence of a vertical magnetic field **B** and rotation (with Ω vertical). $Q^{1/2}$ is proportional to B while $Ta^{1/2}$ is proportional to Ω. Note that both rotation and the magnetic field reduce the efficiency of heat transfer. There is no hint of a cooperative effect of the two in this regime. (Reprinted with permission from Aurnou, J. M. and Olson, P. L., "Experiments of Rayleigh–Bénard convection, magnetoconvection and rotating magnetoconvection in liquid gallium," *J. Fluid Mech.* **430**, 283–307 (2001). Copyright (2001) by Cambridge University Press.)

could be more efficient in a rotating sphere if it creates a magnetic field, and hence that dynamo action was the natural expression of convection in a rotating sphere. Furthermore, it was argued that the amplitude of the magnetic field would settle at a level where the Coriolis and Lorentz forces are roughly in balance. These ideas are behind the proposal of a magnetostrophic experimental dynamo by our group in Grenoble (see above). Note that numerical models of convective dynamos only partly support this idea since the heat transfer is enhanced when a magnetic field is present (Christensen *et al.*, 1999; Grote *et al.*, 2000) but the onset of convection does not seem to be lowered (see Busse *et al.* in Chapter 6 of this volume). This discrepancy could be due to the fact that the magnetic field is not imposed in a dynamo, in contrast to the case treated by Chandrasekhar, or to the fact that numerical dynamos are not yet in the small Ekman number limit where his results apply. At any rate, it is clear that Rayleigh–Bénard convection with an imposed magnetic field and rotation is a topic that deserves further investigation. This motivated Aurnou and Olson (2001) to run a comprehensive set of experiments with liquid gallium. The focus was on measuring the Nusselt number (convective heat transfer divided by conductive: the Nusselt number is equal to unity in the absence of convection) for various values of the imposed magnetic field and rotation rate. As shown in Figure 10, Aurnou and Olson found that the measured Nusselt numbers could be simply contoured in the plane that draws a modified Rayleigh number along the x-axis and the logarithm of the Taylor number along the y-axis ($Ta = 4\Omega^2 D^4/\nu^2 = (2/E)^2$ where E is the Ekman number). The modified Rayleigh number $RaQ^{-1/2}$ incorporates the effect of the magnetic field, since Q is the Chandrasekhar number $Q = \sigma B^2 D^2/\rho\nu$. The results indicate that convection is inhibited by the presence of

rotation and by the magnetic field, as expected. In contrast with the experimental results of Nakagawa, there is no indication for a domain in which the simultaneous action of the Lorentz and Coriolis forces lead to an enhancement of convection. However, it should be noted that both rotation and the magnetic field are moderate in these new experiments. The asymptotic regime studied by Chandrasekhar and his followers is therefore not reached. A nice extension of the work of Aurnou and Olson would be to reach these asymptotic regimes and document both the heat transfer and velocity field. The results would be very valuable for understanding convective dynamos at small Prandtl number.

3.2. Thermal convection in a rotating sphere and annulus

The experimental study of thermal convection in a rotating sphere was pioneered by Busse and his coworkers (Carrigan and Busse, 1976). The centrifugal force can mimic the radial gravity of a self-gravitating planet. The sign is reversed, thus the temperature gradient must also be reversed. The fact that the centrifugal acceleration has a cylindrical symmetry is not important as long as one remains in the quasi-geostrophic regime, subject to the constraints of the Proudman–Taylor theorem. The asymptotic analyses of Roberts (1968) and Busse (1970) show that convection takes the form of convective columns with their axis aligned with the axis of rotation. The widths of the columns is proportional to $E^{1/3}$ where E is the Ekman number $E = \nu/\Omega R^2$ (ν is the kinematic viscosity, Ω is the rotation rate and R the radius of the sphere). The importance of the slope ζ of the spherical boundaries at the two ends of the columns was emphasized by Busse, who introduced a model of convection in an annulus with tilted top and bottom boundaries. The tilt is responsible for the development of thermal Rossby waves and bends the columns in a prograde direction. When the tilt varies with cylindrical radius as in the sphere, the period of the Rossby wave varies and produces a prograde spiralization of the columns (see Busse *et al.* in Chapter 6 of this volume). All these phenomena are well characterized in numerical models of convection just above the onset. Experiments have been used to extend the understanding of these phenomena farther away from the onset, and for small Ekman and Prandtl numbers.

3.3. Thermal convection in an annulus filled with a low Prandtl number liquid

Experiments were carried out by Lathrop and his colleagues with liquid sodium in a 20 cm diameter annulus spinning at rotation rates up to 6,000 rpm. By measuring the magnetic field induced in response to a sinusoidal excitation, Peffley *et al.* (2000b) found evidence for four columns at moderate Rayleigh numbers while a turbulent signature was observed at higher Rayleigh numbers. At these low Ekman numbers ($\sim 10^{-7}$), marginal stability theory (Jones *et al.*, 2000) predicts a much larger number of columns, which would probably not be detected in Peffley's experiments. It is not yet clear what causes the signal at lower frequency they observe.

Experiments with mercury and gallium–indium–tin alloy were run in Bayreuth, where the emphasis was on characterizing the onset of convection (Jaletzky, 1999). The liquid is contained in a small-gap cylindrical shell (height, $h = 50$ mm, gap width, $d = 5$ mm; middle radius in the gap, 67 mm) with upper and lower boundaries tilted at 45° ($\zeta = -1$). As predicted by marginal stability analysis, the onset is oscillatory. Rapid temperature oscillations are recorded on thermistors on the walls. However, the comparison of the measured frequencies and critical Rayleigh numbers with the theoretical predictions shows that one must take into account friction in the vertical Ekman boundary layers on the inner and outer cylinders

(Plaut and Busse, 2002). A suitable parameter is the Coriolis parameter $Co = (2\zeta d/h)/E$. For liquids with Prandtl number larger than about 10, dissipation on the vertical walls is negligible once the Coriolis parameter is larger than 10^4, but as the Prandtl number decreases one needs an increasingly large Coriolis parameter for dissipation on the walls to be negligible. In the weakly nonlinear regime for small Prandtl numbers, this theory also predicts a strong retrograde zonal wind, which remains to be searched for in the experiments.

3.4. Thermal convection in a rotating sphere filled with water and gallium

Experiments are well suited for exploring the fully developed convective states, which are difficult to access in numerical models. This route was followed by Cardin and Olson (1994) who studied convection in a sphere filled with water at high Rayleigh numbers. They found that convection becomes turbulent and that columns fill in a large part of the sphere, while their dimensions remain similar to those predicted at the onset. They observe a mean zonal flow, which is retrograde near the inner sphere and can be explained in terms of Reynolds stresses.

Further experiments have been carried out by our team in Grenoble (Aubert *et al.*, 2001). Both water and liquid gallium were used to fill a 22 cm diameter sphere, which is spun up to 800 rpm. Ekman numbers range from 10^{-5} to 10^{-7}, while the Rayleigh number is up to 80 times critical. The Prandtl number Pr of water is 7 and that of gallium is 0.023 (see Table 1). The main objective was to derive scaling relationships in order to better identify physical mechanisms and permit an extrapolation to core conditions. Since gallium is opaque, optical measuring techniques are inappropriate. Therefore, we used ultrasonic Doppler velocimetry to measure convective velocities. Specific protocols were devised and validated for application to gallium (Brito *et al.*, 2001). With this technique, radial profiles of radial velocity are obtained. We also measure the radial profile of average zonal velocity. The most striking observation is that a strong zonal retrograde flow is present in the gallium experiments. Following Cardin and Olson (1994), we attribute this to Reynolds stresses produced by the turbulent convective motions. Typical radial size δ_r and velocity u_r are deduced from the radial profiles of velocity and a local Reynolds number is built as $Re_l = u_r \delta_r / \nu$. While this number is less than 100 in all the water experiments, it reaches 600 in the gallium experiments, even though the Rayleigh number is at most four times critical in gallium. As in classical two-dimensional turbulence, the energy is not dissipated at the convective scale but cascades up to larger scales. In the sphere the only large-scale truly geostrophic motions are the zonal motions. These motions are created by the Reynolds stresses of the convective eddies and their velocity is limited by friction on the outer boundary. Following Cardin and Olson (1994), we developed a quasi-geostrophic turbulent model from which the following scaling relationships are derived:

$$u_r = \frac{\nu}{D^2} \left(\frac{Ra_Q}{Pr^2} \right)^{2/5} E^{1/5}, \tag{3}$$

$$\delta_r = D \left(\frac{Ra_Q}{Pr^2} \right)^{1/5} E^{3/5}, \tag{4}$$

$$\frac{u_{\text{zonal}}}{u_r} = Re_l^{2/3} E^{1/6}, \tag{5}$$

where we introduced the heat flux based Rayleigh number

$$Ra_Q = \frac{\alpha \gamma P D^2}{k \kappa \nu},$$

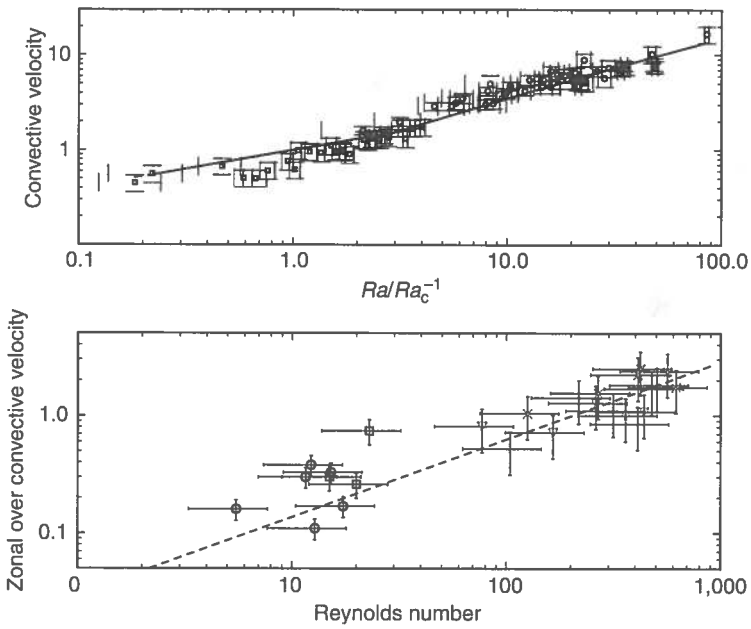

Figure 11 Thermal convection in a rotating sphere filled with water or gallium. Velocities are measured using ultrasonic Doppler velocimetry. Top: nondimensionalized radial velocity as a function of Rayleigh number. All data points [squares for gallium (low Ra) and circles for water (high Ra)] follow the law predicted from a quasi-geostrophic turbulent model (solid line, see text). Bottom: ratio of the zonal to radial velocities increases with the local Reynolds number (see text). Large zonal velocities are measured in the experiments for gallium. (After Aubert *et al.*, 2001.)

in which P is the heat power input, D is the thickness of the spherical shell, α is the coefficient of thermal expansion, k is the thermal conductivity, and γ is the acceleration (due to gravity or to rotation). As shown in Figure 11, these predictions are found to be in excellent agreement with our measurements. These laws can be used to dimension a hypothetical convective dynamo (see above). The large zonal velocities are reminiscent of the observations of Grote *et al.* (2000) for convection in a rotating spherical shell with free-slip boundaries (see Busse *et al.*, Chapter 6). However, we do not observe the intermittency of convection that accompanies this phenomenon in the numerical experiments. It could be because the mechanism that limits the amplitude of the zonal flow is friction at the outer boundary in our experiments while it is probably linked to viscous dissipation in the bulk of the liquid in the numerical experiments. Extrapolating to core conditions, we predict convective and zonal velocities of the order of 1 mm s^{-1}. This is probably one order of magnitude larger than observed (Hulot *et al.*, 1990). Further experiments are under way to explore how an imposed magnetic field modifies the physics and the laws (see Brito *et al.*, 1995). One of the interest of these experiments with liquid metals is that flows are both turbulent (large Reynolds number) and strongly influenced by rotation (small Ekman number). With measurement techniques such as ultrasonic Doppler velocimetry, both the mean flow and the time dependence can be investigated quantitatively, and we may hope to better characterize turbulence in this situation, and with a magnetic field as well, one goal being to parameterize sub-grid turbulence in numerical models of the dynamo.

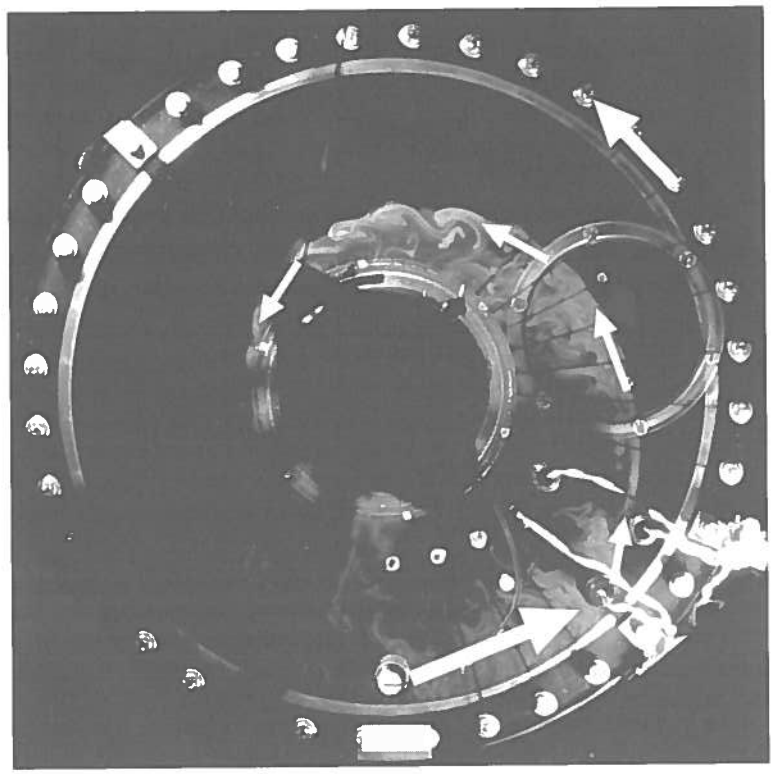

Figure 12 Equatorial planform of rotating hemispherical shell convection with anomalous heat flux at the outer boundary (heater, white rectangle) at $E = 4.7 \times 10^{-6}$, visualized by fluorescent dye. Rotation is anticlockwise. Global locking is observed here for $Ra/Ra_c = 26$ and a peak heat flux sixty-nine times larger than its mean. White dye was injected adjacent to the heater. White arrows indicate induced flows (eastward flow (broad arrow) and a narrow jet along the front (fine arrows)). (Reprinted with permission from Sumita, I. and Olson, P., "A laboratory model for convection in Earth's core driven by a thermally heterogeneous mantle," *Science* **286**, 1547–1549 (1999). Copyright (1999) American Association for the Advancement of Science.)

3.5. Core–mantle coupling

The question of thermal coupling between the core and the mantle has been studied experimentally by Sumita and Olson (1999). Because the time scales are so much larger in the mantle than in the core, and because the temperature fluctuations are very small in the core, the core–mantle boundary is seen as an isothermal boundary from the mantle side and as a boundary with an imposed stationary but spatially variable heat flux from the core side. This thermal inhomogeneity of the outer boundary can play a role on the organization of convective motions in the core. Sumita and Olson performed experiments in a hemisphere filled with water, rotating eastwards around a vertical axis. The thermal anomaly is provided by a narrow heater on the side. When the heat flux anomaly is strong (larger than about 35 times the mean), an interesting global locking is observed. As shown in Figure 12, a spiralling front forms, bordered by a narrow jet, which divides a warm region

to the west from a cold region to the east, preventing mixing between them. The spiralling front originates eastwards of the heater, and a global eastward flow is observed as well. Velocities in the jet are four to five times larger than the eastward flow. Sumita and Olson suggest than fronts and jets could form in the core, in response to heat flux anomalies caused by mantle convection at the core–mantle boundary. These features could influence the dynamo and for example, control the path followed by the virtual paleomagnetic pole during inversions.

3.6. Crystallization experiments and the inner core

Rather unexpectedly, laboratory experiments have also been used to tackle the question of the solidification of the inner core. The goal is to explain the observation that seismic waves travelling through the inner core parallel to the axis of rotation of the Earth are some 4% faster than those that travel perpendicular to it (see Song, 1997 for a review). This is usually attributed to seismic anisotropy due to lattice preferred orientation of iron crystals. There remains to explain why the crystals are consistently aligned with respect to the axis of rotation and to account for the observed level of anisotropy.

The topic was investigated by Bergman (1997, 1998) in a series of papers. Bergman solidified tin–lead alloys under a controlled directional heat flow. He observed that dendrites tend to grow parallel to the heat flow, and correspond to a single crystallographic direction. This direction is ⟨110⟩ for the tin–lead alloy but is predicted to be ⟨210⟩ for iron in the hcp system believed to be favoured at inner core conditions. Bergman also measured ultrasonic wave anisotropy in the solidified alloy and found it to be in agreement with the solidification texturing. The extrapolation to the inner core assumes that heat flow is cylindrically radial so that crystals grow perpendicular to the axis of rotation. This is not incompatible with the organization of convection in vortices aligned with the axis of rotation, which transfer heat more efficiently parallel to the equatorial plane. Under this hypothesis, Bergman could reproduce the variation of seismic velocities as a function of the angle of propagation but found it difficult to account for a level of anisotropy as high as observed. From his experiments, Bergman also inferred that typical iron crystals in the inner core would be hundreds of meter wide and several kilometres long.

A slightly different approach was taken by Brito (1998). With Olson, he solidified a pure metal – gallium – under a directional heat flow and investigated the effect of several different ingredients that could play a role in the core. Using ultrasounds as well, they also found that crystals grow along the heat flow direction but not along a particular crystallographic axis. However, once a given crystallographic direction is present (from small pre-existing crystallites, for example) all crystals tend to grow with the same alignment. All other ingredients – stirring, magnetic field – could not change this behaviour. The extrapolation to the core suggests that a cylindrically radial heat flow is not sufficient to produce lattice preferred orientation in the inner core. Brito proposes that seismic anisotropy rather reflects some primordial crystallographic orientation.

4. Mantle convection

Experiments continue to play an important role in the study of mantle convection. In contrast to core dynamics, the proper nondimensional numbers can now be reached in three-dimensional numerical models of mantle convection. However, there are a number

of complexities either asserted or presumed that are not dealt with easily in numerical models. They include strong variations of material properties, or at the opposite subtle chemical heterogeneities, both possibly leading to some kind of layering. Thermal plumes in a liquid with temperature-dependent viscosity also display specific features, such as oscillations akin to solitons in their conduit, which are suitable to analogical experiments.

4.1. Two-layer convection

In the 1970s, several studies were devoted to convection in two superposed layers (e.g. Richter and Johnson, 1974). At that time, there were clear indications that something was happening at a depth of about 650 km in the mantle, and it was thought that tectonic plates – the surface manifestation of mantle convection – could not subduct below that depth. Hence, the idea that mantle convection was organized in two superposed layers, the 650 km boundary marking some kind of compositional interface. One important issue was the kind of coupling that could exist between convective structures above and below the interface, and two end members were identified: 'mechanical coupling', when cold downwellings in the upper layer lie above hot uprisings in the lower layer, and 'thermal coupling' when hot uprisings in the two layers are superposed, yielding a large shear between cells at the interface (Cserepes *et al.*, 1988; Cardin *et al.*, 1991). Ten years later, it was clear that the 650 km seismic discontinuity was almost entirely due to a mineralogical phase transition rather than to compositional layering (although some questions have arisen recently (Hirose *et al.*, 2001)), and seismic tomography provided evidence that subducting slabs could penetrate the 650 km discontinuity and even reach the core–mantle boundary. However, the topic has been revived recently with emphasis on convection in layers that differ by a very small compositional difference. It is indeed plausible that the D″ layer or some part of the lower mantle has a slightly different chemical composition than the rest of the mantle. The density difference between the two layers would be very small and the interface would be widely distorted by convective motions. The situation is not easily dealt with in numerical models but can be investigated in the laboratory. A thorough investigation was carried out by Davaille (1999a) who superposed two miscible viscous liquids and varied the ratios between the densities, the viscosities, the depths and the vigour of convection. She observed several different regimes, depending mostly on the density ratio. Figure 13 displays two experiments with a strong density ratio (top) and a small density ratio (bottom). In the first case, the interface between the two layers is rather flat on average, but thin filaments of the opposite fluid are entrained on both sides. When the density ratio is weak, the interface is widely distorted and layers form diapirs that can extend all the way to the opposite boundary. In addition, the system can evolve with time from the first to the second situation since the density ratio between the two layers decreases as mixing proceeds. Davaille (1999b) noted that the features she observed are reminiscent of some geophysical observations: the thin filaments entrained by thermal plumes could explain peculiar geochemical signatures of hotspot basalts, while it is tempting to relate the large diapirs of the second regime with the superswells observed in seismic tomography. One important issue that remains to be further analysed is the role of chemical diffusion in these experiments. The inter-diffusivity of the two liquids is many orders of magnitude larger than chemical diffusivities in the mantle, and it is not completely clear yet how the entrainment process should be scaled. In turn, the experiments suggest that the boundary conditions usually employed in numerical models of layered convection probably oversimplify the real situation.

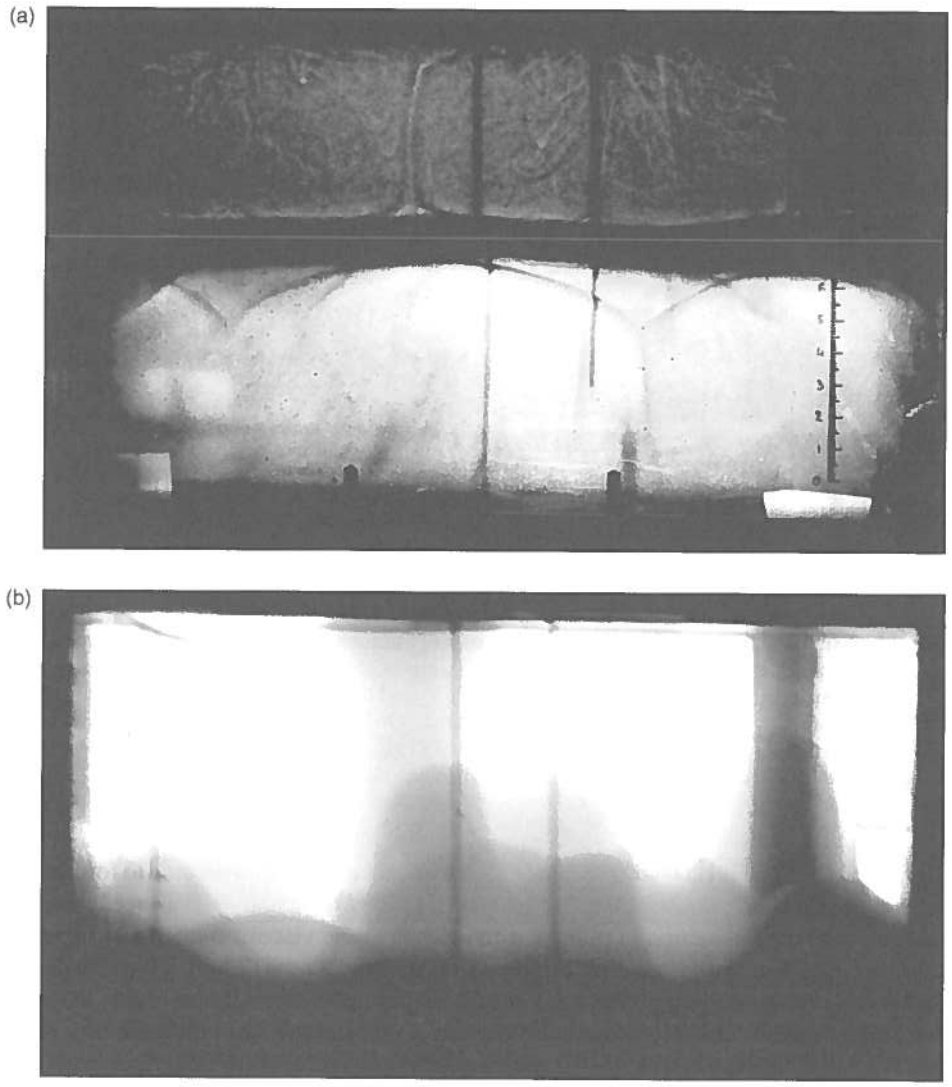

Figure 13 Patterns and entrainment in thermal convection of two superposed miscible liquids. Top: the density ratio of the two liquids is large compared to that of temperature induced variations. Thin filaments are advected away from convergence wedges at the interface. Bottom: the intrinsic density ratio is similar to that of temperature induced variations. Large domes form and can reach the opposite boundary before relaxing back. (Reprinted with permission from Davaille, A., "Simultaneous generation of hotspots and superswells by convection in a heterogenous planetary mantle," *Nature* **402**, 756–760 (1999). Copyright (1999) by *Nature*.) (See Colour Plate XIII.)

4.2. Plumes

Thermal plumes rising in the mantle could have a much lower viscosity than the surrounding mantle. Early experiments (e.g. Whitehead and Luther, 1975; Olson and Singer, 1985;

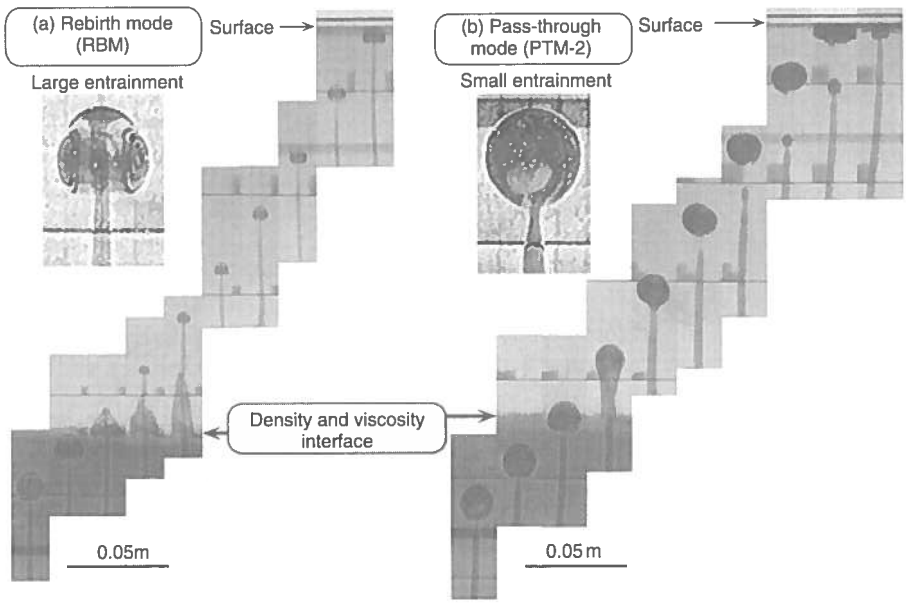

Figure 14 Composite images of the ascent history of a light plume across the interface between two miscible liquids. Two different behaviours are observed depending on the density and viscosity ratios: the rebirth mode (on the left) and the pass-through mode (on the right). (Reprinted from Kumagai, I. and Kurita, K., "On the fate of mantle plumes at density interfaces," *Earth Planet. Sci. Lett.*, **179**, 63–71, Copyright (2000) with permission from Elsevier Science.) (See Colour Plate XII.)

Griffiths and Campbell, 1990) showed that under these conditions, plumes tend to form a large head that rises at almost constant velocity and is fed by a narrow conduit. Recent experiments have dealt with the interaction of plumes with a density (and viscosity) interface. Figure 14 illustrates two different regimes discovered by Kumagai and Kurita (2000). When the density ratio between the ascending plume head and the upper layer is small, the plume is slowed down at the interface and a new plume forms and rises from the stagnating primary plume head. For larger density ratios, the plume is able to pass through the interface with little distortion. In the first mode, the ascent is slow and entrainment of lower layer material is strong in the plume head.

Laudenbach and Christensen (2001) studied another aspect of plume dynamics. They injected hot glucose syrup (whose viscosity depends strongly on temperature) in cold syrup, and looked at the effect of a short enhancement of the injection rate. As illustrated in Figure 15, this produces a solitary conduit wave that propagates along the pre-existing plume conduit. By measuring the deflection of a laser beam, radial temperature profiles in the conduit and in the solitary wave can be obtained. They are found to be in good agreement with numerical models. Laudenbach and Christensen show that these waves have a closed flow structure (the material remains trapped within the wave) similar to that found in compositional plumes. The thermal wave propagates faster than 'normal' material in the plume conduit. It is also hotter and carries more material. Thermal solitary waves could therefore be at the origin of periodic magma production at weak hotspots.

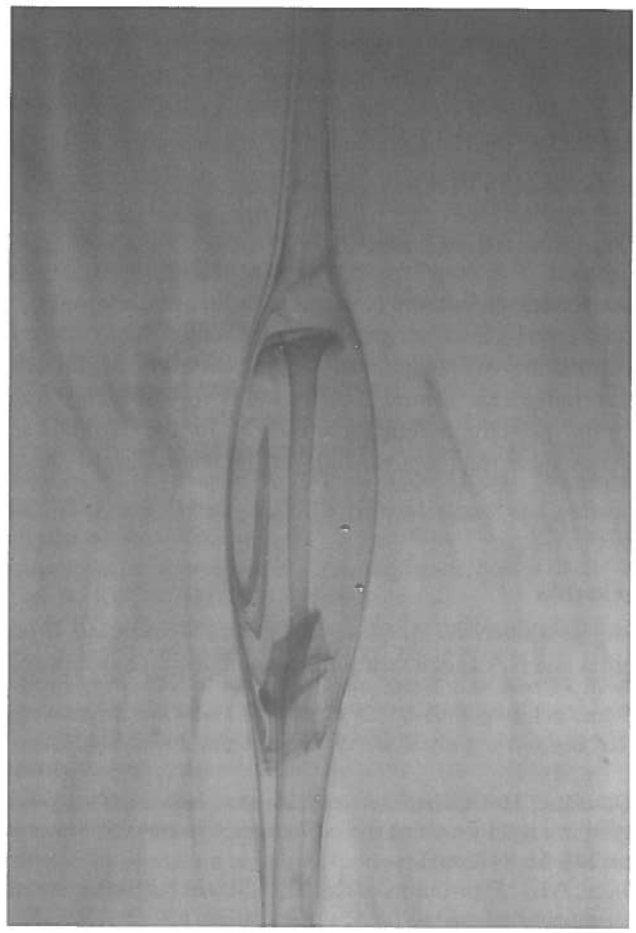

Figure 15 A solitary wave propagating in the conduit of a thermal plume. A sudden increase in the influx rate of a mature plume triggers the formation of a buldge that propagates upward in a solitary wave fashion. Dye is injected in the plume for visualization. (Reprinted with permission from Laudenbach and Christensen, 2001). (See Colour Plate XIV.)

4.3. Convection in a radial force field

Every experimentalist has once dreamed of reproducing in the laboratory the radial gravity field of self-gravitating bodies such as the Earth in order to investigate the effect of spherical geometry on convection. One way of approaching this is to use a hemisphere and spin it at a rotation rate just enough for the centrifugal acceleration at the equator to match the acceleration due to gravity. However, one is limited to a hemisphere and the acceleration equipotentials are not spherical. Nevertheless, this has proven useful in the case of experiments where convection is strongly influenced by rotation (small Ekman number) (Cordero and Busse, 1992; Cordero, 1993; Sumita and Olson, 1999, 2000).

Two other tracks have been recently followed. In both cases, gravity is replaced by another body force.

A group in Bremen is building a spherical shell in which the dielectrophoretic force is driving convection (Egbers *et al.*, 1999). The temperature difference is replaced by a difference in electrical potential between the inner and outer sphere. The experiment is meant to function in space in microgravity, as did the pioneer experiment of Hart *et al.* (1986). The platform of convection will be observed through a clever shadowgraph technique.

An even more far-fetched idea was developed by Rosensweig *et al.* (1999). Specialists of ferrofluids, the researchers of that group filled a spherical shell with ferrofluid and placed a magnet within the inner sphere, surrounded by a heating foil. Under these conditions, convection can take place. The fact that ferrofluids are opaque makes the observation of planforms more difficult. The faint temperature fluctuations caused by convection at the surface were observed using an infrared camera.

Although one is amazed by the deployment of imagination demonstrated in these experiments, it is not clear that they will help understanding better the organization of convection in planetary mantles. Indeed, the central acceleration is very different from that of planets: it decays as r^{-5} for the dielectrophoretic force and r^{-4} for the ferrofluid set-up (where r is radius), while it is constant in the Earth's mantle and increases almost linearly with radius in the core.

5. Acknowledgements

I thank G. Gerbeth, U. Müller, R. Stieglitz, D. Lathrop, J. Aurnou, J. Aubert, I. Sumita, A. Davaille, K. Kurita and N. Laudenbach for providing the figures reprinted in this review.

References

Aubert, J., Brito, D., Nataf, H.-C., Cardin, P. and Masson, J.-P., "Scaling relationships for finite amplitude convection in a rapidly rotating sphere, from experiments with water and gallium," *Phys. Earth Planet. Inter.* **128**, 51–74 (2001).

Aurnou, J. M. and Olson, P. L., "Experiments on Rayleigh–Bénard convection, magnetoconvection and rotating magnetoconvection in liquid gallium," *J. Fluid Mech.* **430**, 283–307 (2001).

Bergman, M. I., "Measurements of elastic anisotropy due to solidification texturing and the implications for the Earth's inner core," *Nature* **389**, 60–63 (1997).

Bergman, M. I., "Estimates of the Earth's inner core grain size," *Geophys. Res. Lett.* **25**, 1593–1596 (1998).

Bourgoin, M., Marié, L., Petrelis, F., Burguete, J., Chiffaudel, A., Daviaud, F., Fauve, S., Odier, P., Pinton, J.-F., "MHD measurements in the von Kármán sodium experiment," *Phys. Fluids* **14** (9), 3046 (2001).

Brito, D., "Approches expérimentales et théoriques de la dynamique du noyau terrestre," *Thèse Université Paris* 7, Janvier 1998.

Brito, D., Cardin, P., Nataf, H.-C. and Marolleau, G., "Experimental study of a geostrophic vortex of gallium in a transverse magnetic field," *Phys. Earth Planet. Inter.* **91**, 77–98 (1995).

Brito, D., Nataf, H.-C., Cardin, P., Aubert, J. and Masson, J.-P., "Ultrasonic Doppler velocimetry in liquid gallium," *Exp. Fluids* **31**, 653–663 (2001).

Bullard, E. C. and Gellman, H., "Homogeneous dynamos and terrestrial magnetism," *Phil. Trans. R. Soc. Lond.* A **247**, 213–278 (1954).

Busse, F. H., "Thermal instabilities in rapidly rotating systems," *J. Fluid Mech.* **44**, 441–460 (1970).

Busse, F. H., Müller, U., Stieglitz, R. and Tilgner, A., "Spontaneous generation of magnetic fields in the laboratory," In: *Evolution of Spontaneous Structures in Dissipative Continuous Systems* (Eds F. H. Busse and S. C. Müller), pp. 546–558. Springer, New York (1998a).

Busse, F. H., Grote, E. and Tilgner, A., "On convection driven dynamos in rotating spherical shells," *Stud. Geophys. Geod.* **42**, 1–6 (1998b).

Cardin, P. and Olson, P., "Chaotic thermal convection in a rapidly rotating spherical shell: consequences for flow in the outer core," *Phys. Earth Planet. Inter.* **82**, 235–239 (1994).

Cardin, P., Nataf, H.-C. and Dewost, P., "Thermal coupling in layered convection: evidence for an interface viscosity control from mechanical experiments and marginal stability analysis," *J. Phys. II* **1**, 599–622 (1991).

Cardin, P., Brito, D., Jault, D., Nataf, H.-C. and Masson, J.-P., "Towards a rapidly rotating liquid sodium dynamo experiment," *Magnetohydrodynamics* **38**, 177–189 (2002).

Carrigan, C. R. and Busse, F. H., "Laboratory simulation of thermal convection in rotating planets and stars," *Science* **191**, 81–83 (1976).

Chandrasekhar, S., *Hydrodynamic and Hydromagnetic Stability*. Oxford University Press, Oxford (1961).

Christensen, U., Olson, P. and Glatzmaier, G. A., "Numerical modelling of the geodynamo: a systematic parameter study," *Geophys. J. Int.* **138**, 393–409 (1999).

Colgate, S. A., Li, H. and Pariev, V., "The origin of the magnetic fields of the universe: the plasma astrophysics of the free energy of the universe," *Phys. Plamas* **8**, 2425–2431 (2001a).

Colgate, S. A., Beckley, H. F., Pariev, V. I., Finn, J. M., Li, H., Weatherall, J. C., Romero, V. D., Westpfahl, D. J. and Ferrel, R., "The New Mexico liquid sodium α–Ω experiment," http://kestrel.nmt.edu/ dynamo/ (2001b).

Cordero, S., "Experiments on convection in a rotating hemispherical shell: transition to chaos," *Geophys. Res. Lett.* **20**, 2587–2590 (1993).

Cordero, S. and Busse, F. H., "Experiments on convection in rotating hemispherical shells: transition to a quasi-periodic state," *Geophys. Res. Lett.* **19**, 733–736 (1992).

Cowling, T. G., "The magnetic field of sunspots," *Mon. Not. R. Astr. Soc.* **94**, 39–48 (1934).

Cserepes, L., Rabinowicz, M. and Rosemberg-Borot, C., "3-dimensional infinite Prandtl number convection in one and 2 layers with implications for the Earth gravity-field," *J. Geophys. Res.* **93**, 12009–12025 (1988).

Davaille, A., "Two-layer thermal convection in miscible viscous fluids," *J. Fluid Mech.* **379**, 223–253 (1999a).

Davaille, A., "Simultaneous generation of hotspots and superswells by convection in a heterogenous planetary mantle," *Nature* **402**, 756–760 (1999b).

Dudley, M. L. and James, R. W., "Time-dependent kinematic dynamos with stationary flows," *Proc. R. Soc. Lond.* A **425**, 407–429 (1989).

Egbers, C., Brasch, W., Sitte, B., Immohr, J. and Schmidt, J. R., "Estimates on diagnostic methods for investigations of thermal convection between spherical shells in space," *Meas. Sci. Technol.* **10**, 866–877 (1999).

Elsasser, W. M., "Induction effects in terrestrial magnetism. 1. Theory," *Phys. Rev.* **69**, 106–116 (1946).

Fearn, D. R., "The geodynamo," In: *Earth's Deep Interior* (Ed. D. J. Crossley), *The Fluid Mechanics of Astrophysics and Geophysics*, **7**, pp. 79–114. Gordon and Breach, New York (1998).

Forest, C., "Madison dynamo experiment," http://aida.physics.wisc.edu/ (1998).

Frick, P., Denisov, S., Khripchenko, S., Noskov, V., Sokoloff, D., Stepanov, R. and Sukhanovsky, A., "A nonstationary dynamo experiment (current state of Perm project)," In: *Proceedings of the Fourth International Pamir Conference*, Presqu'île de Giens, pp. 183–188. France (2000).

Gailitis, A. and Freibergs, J., "Theory of a helical MHD dynamo," *Magnetohydrodynamics* **12**, 127–129 (1976).

Gailitis, A., Karasev, B. G., Kirillov, I. R., Lielausis, O. A., Luzhanskii, S. M., Ogorodnikov, A. P. and Preslitskii, G. V., "Liquid metal MHD dynamo model experiment," *Magnetohydrodynamics* **23**, 349–353 (1987).

Gailitis, A., Lielausis, O., Dement'ev, S., Platacis, E., Cifersons, A., Gerbeth, G., Gundrum, T., Stefani, F., Christen, M., Hänel, H. and Will, G., "Detection of a flow induced magnetic field eigenmode in the Riga dynamo facility," *Phys. Rev. Lett.* **84**, 4365–4368 (2000).

Gailitis, A., Lielausis, O., Platacis, E., Dement'ev, S., Cifersons, A., Gerbeth, G., Gundrum, T., Stefani, F., Christen, M. and Will, G., "Magnetic field saturation in the Riga dynamo experiment," *Phys. Rev. Lett.* **86**, 3024–3027 (2001).

Glatzmaier, G. A., "Numerical simulations of a convective dynamo experiment," In: *SEDI 2000*, The 7th symposium of Study of the Earth's Deep Interior, Exeter, UK, Abstract S5.7 (2000).

Griffiths, R. W. and Campbell, I. H., "Stirring and structure in mantle starting plumes," *Earth Planet. Sci. Lett.* **99**, 66–78 (1990).

Grote, E., Busse, F. H. and Tilgner, A., "Regular and chaotic spherical dynamos," *Phys. Earth Planet. Inter.* **117**, 259–272 (2000).

Hart, J. E., Glatzmaier, G. A. and Toomre, J., "Space-laboratory and numerical simulations of thermal convection in a rotating hemispherical shell with radial gravity," *J. Fluid Mech.* **173**, 519–544 (1986).

Herzenberg, A., "Geomagnetic dynamos," *Phil. Trans. R. Soc. Lond.* A **250**, 543–585 (1958).

Hirose, K., Fei, Y., Ono, S., Yagi, T. and Funakoshi, K.-I., "In situ measurements of the phase transition boundary in $Mg_3Al_2Si_3O_{12}$: implications for the nature of the seismic discontinuities in the Earth's mantle," *Earth Planet. Sci. Lett.* **184**, 567–573 (2001).

Hulot, G., Le Mouël, J.-L. and Jault, D., "The flow at the core–mantle boundary: symmetry properties," *J. Geomagn. Geoelectr.* **42**, 857–874 (1990).

Jaletzky, M. U., "Über die Stabilität von thermisch getriebenen Strömungen im rotierenden konzentrischen Ringspalt," Doktorat Universität Bayreuth (1999).

Jault, D., Nataf, H.-C. and Cardin, P., "Feasability study of a dynamo experiment in the magnetostrophic regime," In: *SEDI 98*, the 6th Symposium of Study of the Earth's Deep Interior, Tours, France, Abstract S7.9 (1998).

Jones, C. A., Soward, A. M. and Mussa, A. I., "The onset of thermal convection in a rapidly rotating sphere," *J. Fluid Mech.* **405**, 157–179 (2000).

Kumagai, I. and Kurita, K., "On the fate of mantle plumes at density interfaces," *Earth Planet. Sci. Lett.* **179**, 63–71 (2000).

Larmor, J., "How could a rapidly rotating body such as the Sun become a magnet?" *Brit. Assn. Adv. Sci. Rep.* **1919**, 159–160 (1919).

Laudenbach, N. and Christensen, U. R., "An optical method for measuring temperature in laboratory models of mantle plumes," *Geophys. J. Int.* **145**, 528–534 (2001).

Lielausis, O., "Dynamo theory and liquid-metal MHD experiments," *Astron. Nachr.* **315**, 303–317 (1994).

Lowes, F. J. and Wilkinson, I., "Geomagnetic dynamo: a laboratory model," *Nature* **198**, 1158–1160 (1963).

Lowes, F. J. and Wilkinson, I., "Geomagnetic dynamo: an improved laboratory model," *Nature* **219**, 717–718 (1968).

Nakagawa, Y., "Experiments on the instability of a layer of mercury heated from below and subject to the simultaneous action of a magnetic field and rotation," *Proc. R. Soc. Lond.* A **242**, 81–88 (1957).

Nakagawa, Y., "Experiments on the instability of a layer of mercury heated from below and subject to the simultaneous action of a magnetic field and rotation II," *Proc. R. Soc. Lond.* A **249**, 138–145 (1958).

Olson, P. and Singer, H., "Creeping plumes," *J. Fluid Mech.* **158**, 511–531 (1985).

Peffley, N. L., Cawthorne, A. B. and Lathrop, D. P., "Toward a self-generating magnetic dynamo: the role of turbulence," *Phys. Rev. E* **61**, 5287–5294 (2000a).

Peffley, N. L., Goumilevski, A. G., Cawthorne, A. B. and Lathrop, D. P., "Characterization of experimental dynamos," *Geophys. J. Int.* **142**, 52–58 (2000b).

Plaut, E. and Busse, F. H., "Low-Prandtl-number convection in a rotating cylindrical annulus," *J. Fluid Mech.* **464**, 345–363 (2002).

Ponomarenko, Y. B., "Theory of the hydromagnetic generator," *J. Appl. Mech. Tech. Phys.* **14**, 775–778 (1973).

Rädler, K.-H., Apstein, E., Rheinhardt, M. and Schüler, M., "The Karlsruhe dynamo experiment. A mean field approach," *Stud. Geophys. Geod.* **42**, 224–231 (1998).

Richter, F. M. and Johnson, J. E., "Stability of a chemically layered mantle," *J. Geophys. Res.* **79**, 1635–1639 (1974).

Roberts, G. O., "Dynamo action of fluid motions with two-dimensional periodicities," *Phil. Trans. R. Soc. Lond.* A **271**, 411–454 (1972).

Roberts, P. H., "On the thermal instability of a rotating fluid sphere containing heat sources," *Phil. Trans. R. Soc. Lond.* A **263**, 93–117 (1968).

Roberts, P. H. and Glatzmaier, G. A., "Geodynamo theory and simulations," *Rev. Mod. Phys.* **72**, 1081–1123 (2000).

Rosensweig, R. E., Browaeys, J., Bacri, J.-C., Zebib, A. and Perzynski, R., "Laboratory study of spherical convection in simulated central gravity," *Phys. Rev. Lett.* **83**, 4904–4907 (1999).

Song, X., "Anisotropy of the Earth's inner core," *Rev. Geophys.* **35**, 297–314 (1997).

Stieglitz, R. and Müller, U., "Experimental demonstration of a homogeneous two-scale dynamo," *Phys. Fluids* **13**, 561–564 (2001).

Sumita, I. and Olson, P., "A laboratory model for convection in Earth's core driven by a thermally heterogeneous mantle," *Science* **286**, 1547–1549 (1999).

Sumita, I. and Olson, P. L., "Laboratory experiments on high Rayleigh number thermal convection in a rapidly rotating hemispherical shell," *Phys. Earth Planet. Inter.* **117**, 153–170 (2000).

Sweet, D., Ott, E., Antonsen, Jr, T. M. and Lathrop, D. P., "Blowout bifurcations and the onset of magnetic dynamo action," *Phys. Plasmas* **8**, 1944–1952 (2001).

Tilgner, A., "A kinematic dynamo with a small scale velocity field," *Phys. Lett.* A **226**, 75–79 (1997).

Tilgner, A., "Towards experimental fluid dynamos," *Phys. Earth Planet. Inter.* **117**, 171–177 (2000).

Tilgner, A. and Busse, F. H., "Saturation mechanism in a model of the Karlsruhe dynamo," In: *Dynamo and Dynamics, a Mathematical Challenge* (Eds P. Chossat, D. Armbouster and I. Oprea) NATO Sci. Ser. II Mathematics, Physics and Chemistry **26**, pp. 153–161. Kluwer Academic Publishers, Dordrecht (2001).

Whitehead, J. A. and Luther, D. S., "Dynamics of laboratory diapir and plume models," *J. Geophys. Res.* **80**, 705–717 (1975).